Asian Journal of Civil Engineering (2022) 23:531–549
https://doi.org/10.1007/s42107-022-00440-0

ORIGINAL PAPER

Investigating applicability of sawdust and retro-reflective materials as external wall insulation under tropical climatic conditions

P. M. Dharmasena[1] · D. P. P. Meddage[2] · A. S. M. Mendis[3]

Received: 27 December 2021 / Accepted: 2 April 2022 / Published online: 19 April 2022

Abstract

Buildings require energy to maintain their performance. In consequence, built environments cause a surge in the world's energy demand. Providing passive measures is an effective method of optimizing operational energy usage. In this study, we propose insulation materials (thermal barrier type and resistive insulation) for the walls of a building. Experiments were performed on small-scale physical models constructed with; (a) no insulation, (b) sawdust–cement mortar, and (c) retro-reflective (RR) material for external walls. In addition, regression models were developed to predict indoor air temperature with insulation. Subsequently, associated operational energy-saving and decrease in emissions were estimated for each material. The comparison reveals RR (sawdust–cement mortar) is effective in warm (overcast) climatic conditions. Developed regression models have shown a good agreement with experimental results ($R > 0.8$). Moreover, sawdust–cement mortar (RR) materials contributed a 9% (13.4%) reduction in operational energy and a 9% (13.3%) decrease in CO_2 emissions. The project highlights the potential to utilize sawdust—a waste material—and RR material as wall insulation to decrease intense operational energy demand.

Keywords Wall insulation · Sawdust · Retro-reflective material · Model house · Regression model · Tropical climate

Abbreviations

A/C	Air conditioning
CO_2	Carbon dioxide
HVAC	Heating ventilation and air conditioning
RR	Retro-reflective
RH	Relative humidity
M1	Model house without any insulation
M2	Model house insulted with sawdust and cement
M3	Model house insulated with RR tape
h	Hours
BTU	British thermal unit
K_1	Thermal conductivity of composite material sawdust and cement insulation
$K_{sawdsut}$	Thermal conductivity of sawdust
$K_{cement\text{-}grout}$	Thermal conductivity of cement grout
$Ø$	Volume fraction of cement grout.
R^2	Coefficient of determination
R	Correlation coefficient
MAE	Mean absolute error
RMSE	Root mean square error
T_P	Predicted indoor air temperature
T_E	Experimental indoor air temperature
$\overline{T}_E$	Mean value of data set
N	Total number of readings

✉ D. P. P. Meddage
meddagedpp.20@uom.lk

[1] Department of Civil Engineering, Faculty of Engineering, Sri Lanka Institute of Information Technology, Malabe, Sri Lanka

[2] Department of Civil and Environmental Engineering, Faculty of Engineering, University of Ruhuna, Hapugala, Sri Lanka

[3] Department of Civil Engineering, Faculty of Engineering, General Sir John Kotelawala Defense University, Ratmalana, Sri Lanka

Introduction

Buildings heavily contribute to the energy demand of the world. Though, the energy performance of buildings has not been reasonably advanced. In consequence, substantial operational energy is required to provide a good microclimate inside a building (Rosas-Flores & Rosas-Flores, 2020). These conditions are strongly dependent on factors such as materials, orientation, and natural ventilation. The present

study focuses on aspects related to building materials. For example, conventional materials (e.g., concrete, cement sand blocks) overlook the requirement of energy efficiency. Therefore, energy-intensive active measures such as A/Cs are often utilized to maintain occupant comfort (Halwatura, 2014).

Annibaldi et al. (2019) reported industrial and urban activities consumed 80% of the world's energy. In addition, Zhang and Yang (2018) stated (23–50%) of energy demand is for buildings. Further, Annibaldi et al. (2021) agree that almost half of global energy is required for the construction sector. Thus, it reveals the possibility of the building sector dominating the prevailing energy crisis in the globe (Lin & Liu, 2015). Building-related energy is primarily categorized into embodied and operational energy components. Embodied component involves energy usage up to the completion of a building (Dissanayake et al., 2009), whereas operational components last throughout the life span. According to Asdrubali et al. (2013), Rossi et al. (2012), and Sartori and Hestnes (2007) energy usage is strongly dependent on the operational stage of a building.

Given previous quantifications, Rosas-Flores and Rosas-Flores (2020), Haik et al. (2020), and Tettey et al. (2014) indicated that 40% of energy in the world is for buildings. In addition, 40% of the above demand is accounted for operational carbon and operational energy (Haik et al., 2020). Dear et al. (2013) highlighted that 38.9% of energy in the United States of America is used for construction and 34.8% is used to increase thermal comfort in the operational stage. Rosas-Flores and Rosas-Flores (2020) further provided that the energy consumption of Mexican houses were increased by 22.4% from 1994 to 2015. Khoukhi (2018) stated that buildings mainly use energy for Heating Ventilation, and Air Conditioning (HVAC) systems. Therefore, it highlights the inferior thermal performance of conventional materials and their subsequent effect on desired micro-climatic conditions (Al-Tamimi et al., 2020; Andiç-Çakir et al., 2021; Halwatura & Jayasinghe, 2008).

According to Mallik (1996), people install air conditioning as a result of adverse micro-climatic conditions, particularly in the daytime. In Mexico, A/C's usually account for 19% of total energy (Rosas-Flores & Rosas-Flores, 2020). In harsh climatic conditions, buildings can account for more than 70% of the total energy requirement for HVAC systems (Khoukhi, 2018). Generally, massive energy demand is coupled with conditioned spaces, thus contributing to greenhouse emissions (Vera et al., 2017). Given no controlling sequence, the average temperature of the earth is expected to increase 1.1–6.4 °C by end of the year 2100 (Aditya et al., 2017). Passive and active measures are implemented to increase thermal comfort (Wang et al., 2019). Passive measures assist to reduce heat gain by improving heat insulation attributes. Active measures majorly consist of energy-based recovery techniques to achieve thermal sensation (e.g., A/C, heating, and mechanical ventilation). As previously highlighted, passive measures are preferred to minimize adverse micro-climatic conditions in contrast to active measures.

Roofs, walls, and openings are major components that transfer solar radiation to buildings. Leo Samuel et al. (2017) recommended having a decreased windows/walls ratio will reduce the cooling requirement. Many researchers emphasized passive techniques to prevent heat absorbance towards building through conduction, convection, and radiation at the design stage. orientation (Meng et al., 2016), thermal insulation, and shading for building (Leo Samuel et al., 2017; Dudzińska & Kotowicz, 2015) promptly influence the daytime energy demand of a building. According to Rosas-Flores and Rosas-Flores (2020), the Mexican government spends more than two billion dollars annually on electricity as a result of the lack of heat insulation. Thermal insulations could be inorganic or organic materials that slow down heat transfer (Khoukhi, 2018). In harsh climatic regions, insulation is vital to reduce thermal discomfort (Rosas-Flores & Rosas-Flores, 2020). Insulation materials have been used effectively in the building sector to reduce energy consumption and environmental impacts (Barrau et al., 2014; Biswas et al., 2016; Braulio-Gonzalo & Bovea, 2017; Streimikiene et al., 2020). Khoukhi (2018) reported that energy can be saved up to 50% of a building, using proper insulation. Because insulation materials can increase resistance to heat flow through the building envelope. It will use less energy in HVAC systems to sustain thermal sensation for occupants (Barrau et al., 2014). In essence, Sun et al. (2018), Dudzińska and Kotowicz (2015), Meng et al. (2016), Leo Samuel et al. (2017), and Sair et al. (2019) stated the significance of comprising materials with high heat capacity, high heat accumulation ability, high ultraviolet reflectivity, and a minor heat transfer coefficient to prevent a building from overheating.

In past, insulated components were rarely used in the Sri Lankan housing sector. However, recent occasions are noticed that proposes insulation for roof slabs to minimize massive heat gain during daytime (Halwatura & Jayasinghe, 2009; Meddage & Jayasinghe, 2022; Nandapala & Halwatura, 2016). However, insulating external walls can provide added benefits to improve the built environment, especially during the daytime. Because Sri Lanka is a tropical country that is exposed to direct solar radiation around 8–10 h per day (Wijesena & Amarasinghe, 2018).

Thereby, the following requirements, materials, and their properties were tabulated to identify the most potent materials (refer to Annex 05). Subsequently, each material was categorized according to usage (e.g., walls, roof, floors, windows, etc.). Insulation materials that we propose for walls were selected from tabulated properties. Considering the aspects (e.g., thermal properties, local availability,

construction convenience, and cost of materials), 'Sawdust' and 'RR' were selected as insulation and thermal barrier type materials, respectively. Sawdust is mixed with cement to prepare sawdust–cement mortar. RR is locally available in tape form. Table 1 presents the properties of materials used in this study.

Sawdust is a waste material that can be collected from the carpentry industry. According to Braulio-Gonzalo and Bovea (2017) and Cetiner and Shea (2018), natural products are hardly used as insulation materials in the construction sector. The authors identify it as a research gap in the building industry. Such plant-based materials reduce embodied carbon dioxide of a building (Cetiner & Shea, 2018; Haik et al., 2020). Generally, sawdust waste is dumped in open areas (Gopinath et al., 2015), and burning leads to emitting greenhouse fumes (Oluyamo & Bello, 2014). Adhering to the concept of circular economy (industrial symbiosis), sawdust can be used as a raw material in construction. It will eventually eliminate waste and pollution that occurs as a result of byproducts of the wood industry. Interestingly, Oluyamo and Bello (2014), Madrid et al. (2018) experimentally confirmed insulation characteristics of sawdust. It has low embodied energy, good sound, and thermal insulation due to its high porosity (Claudiu, 2014; Hafed, 2017). Subsequently, Hafed (2017) has found that the use of sawdust in cement mortar possesses a lower thermal conductivity and lower density compared to traditional cement mortar.

There are four types of RR materials, namely Glass bead RR materials, Capsule RR materials, Prism RR materials, and Transparent RR materials (Wang et al., 2021). The original purpose of RR materials was to improve traffic signs and safety clothing (Yuan et al., 2016). Manni et al. (2018) and Castellani et al. (2020) reported that RR materials contain reflective properties. Thus, RR materials can be applied for buildings as a coating to reduce heat-island effects and the thermal load of a building. Meng et al. (2016) confirmed that RR materials reduce internal surface temperature and indoor air temperature by 8–10 °C and external wall temperatures by 10–20 °C. Further, Meng et al. (2015) showed that RR material reduces the air temperature of a prefabricated house by more than 7 °C. Yoshida et al. (2014), reported that a 23% decrease in energy consumption was obtained as a result of applying RR materials to windows. Zhang et al. (2017) used prism type (59% reflectivity) RR materials to walls. Accordingly, they observed a 15.2% reduction in cooling load with respect to a building without RR material. Xu et al. (2020) proposed RR materials (62.3% reflectivity) for tents as a result of a 10.4% reduction in total energy consumption. We suggested 3M Diamond Grade (White color) DG Reflective Sheeting Series 4000 for the study. However, the authors highlight the lack of thermal properties of this material in previous studies.

Hence, this study was initiated with the following objectives: (a) to investigate heat insulation performance of sawdust and RR material; (b) to develop a mathematical model to predict indoor air temperature for respective insulation materials; (c) to estimate operational energy-saving due to insulated walls; (d) to estimate emission reductions associated with decreased energy utilization. To achieve objectives, both experimental and analytical modeling was performed. The authors constructed small-scale physical models for the field experiments. Subsequently, mathematical models were developed using the R-studio platform to predict the indoor air temperature of insulated model houses. Ridge regression models were used to obtain predictions. Finally, cost and emission analyses were performed to evaluate insulation in terms of operational energy aspects.

Methodology

Field experiment

For experiment, three small-scale physical models were constructed which are 0.9 m (length) × 0.9 m (width) × 0.9 m (height). Asbestos sheets were provided as roofing (1 × 1 m). All models were provided with a 0.3 m (height) × 0.3 m (width) opening in the front wall to facilitate air movement inside a real building. The front wall faces the North direction, minimizing heat gain due to solar radiation. Further,

Table 1 Properties of selected materials for the study

Name of material	Thermal conductivity (W/m K)	Solar reflectance (albedo value)	Specific heat capacity (J/kg K)	Density (kg/m^3)
Solid brick (for walls)	0.77 (Dudzińska & Kotowicz, 2015)	–	880 (Dudzińska & Kotowicz, 2015)	1800 (Dudzińska & Kotowicz, 2015)
Asbestos sheet (for roof)	0.4733 (Ariyadasa et al., 2015)	–	–	1630 (Ariyadasa et al., 2015)
RR tape (wall insulation)	2.026 (Meng et al., 2016)	0.81 (Yuan et al., 2015)	1324 (Meng et al., 2016)	307 (Meng et al., 2016)
Sawdust (Wall insulation)	0.038–0.050 (Schiavoni et al., 2016)	-	1900–2100 (Schiavoni et al., 2016)	50–270 (Schiavoni et al., 2016)

these openings are required to mount equipment and sensors inside the model during the experiment. Standard engineering clay bricks were used to construct the model house structure. Wall thickness was maintained as 0.2 m for all three model houses. For the M2 model, the sawdust–cement mortar was applied on external walls. A ratio of 1:3 (cement: sawdust) was used to prepare mortar whereas plaster thickness was kept as 25 mm. For the M3 model, RR tapes (white color diamond grade) were stuck on external walls as insulation. No insulation was provided for the control model (M1), adhering to conventional construction practice in Sri Lanka. Figure 1 depicts constructed models and cross-sectional arrangements (a) Model house without any insulation (M1); (b) Model house insulated with sawdust and cement mortar (M2); (c) Model house insulated with RR tape (M3).

A hygrometer was used to measure the indoor air temperature (°C), outdoor air temperature (°C), and relative humidity (RH) (%) with a sensitivity of ± 1.0 °C, ± 5 RH. Outer and inner surface temperature (°C) in each direction (North, East, South, and West) walls were measured using a thermometer with a sensitivity of ± (1% + 4). All temperature readings were recorded from 6.00 a.m. to 6.00 p.m. in hourly intervals. Temperature and relative humidity readings were collected for sunny weather conditions and overcast sky conditions, respectively. Readings were taken for five days in each condition and critical two days were chosen for analysis. Temperature readings were not recorded during rain in overcast sky conditions. Outer and inner surface temperature readings were obtained from four locations as shown in Fig. 1. Next, the arithmetic average was obtained by using four readings per surface.

Thermal conductivity calculation of sawdust and cement insulation

Since external walls of the M2 model house were insulated with sawdust–cement mortar, thermal conductivity for composite material should be estimated. Progelhof et al. (1976) provided an equation (Eq. 1) to estimate the thermal conductivity of a composite material. K_1 denotes thermal conductivity of composite material sawdust and cement insulation, K_{sawdsut} represents thermal conductivity of sawdust, $K_{\text{cement-grout}}$ represents thermal conductivity of cement grout and Ø is the volume fraction of cement grout.

$$\frac{1}{K_1} = \frac{1-\infty}{K_{\text{Sawdust}}} + \frac{\infty}{K_{\text{Cement-grout}}}. \tag{1}$$

Regression models

Regression models were developed based on experimental observations to predict indoor air temperature. Sunny sky readings were used to develop regression models since overcast sky conditions had disrupted air temperature readings. Since there are multiple independent variables, simple linear

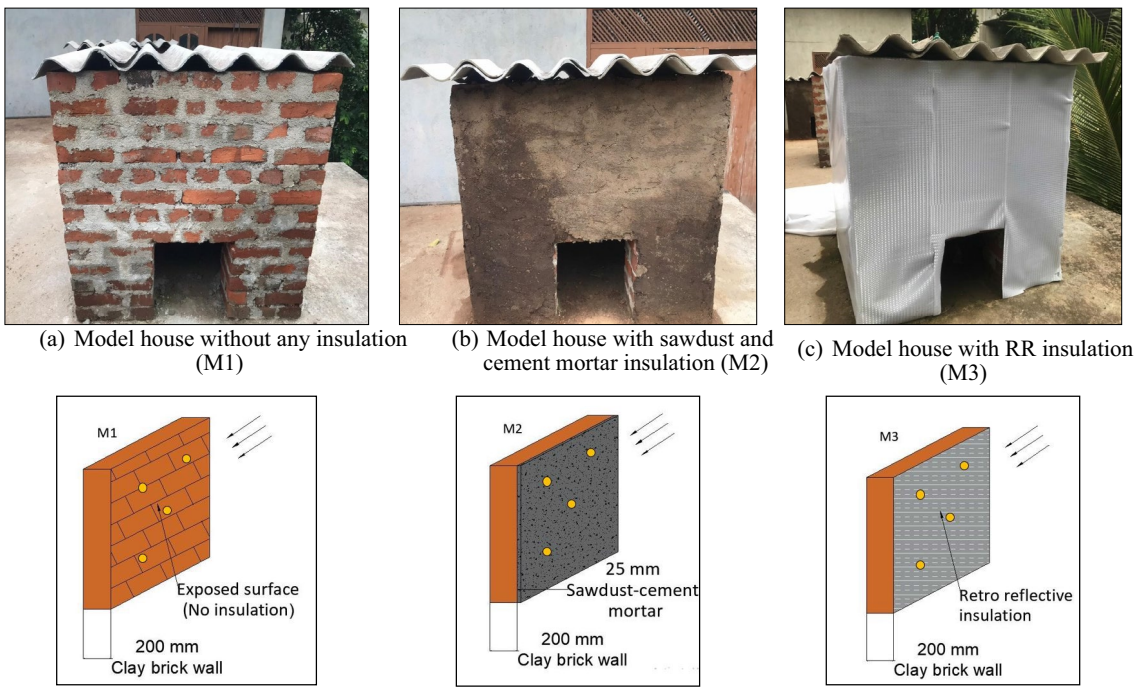

Fig. 1 Constructed small-scale physical models and corresponding section arrangement of walls (Of note that yellow markers denote the locations of sensors)

regression cannot be employed for this purpose. However, the complexity of the equation was decided to be lower, hence, multiple linear regression is the subsequent option. Multiple linear ridge regression (James et al., 2017) was used for the study, which is based on linear least squares regression on the R-studio platform. When the training data set is fed into R-studio, the regression technique (multiple-linear) determines the appropriate coefficients. Later, the validation (*unseen data*) set is employed to evaluate the performance of obtained models.

The working principle of ridge regression is to shrink coefficients or weights towards zero. It is obtained through imposing a suitable penalty. On other hand, ridge regression is an extended version of linear regression in which complexity is minimized through loss function. Afterward, 75% of experimental data was fed to the training sequence of the model whereas the remaining 25% was kept for the validation process. The equation that we propose holds ($Y = m_1 X_1 + m_2 X_2 + m_3 X_3 + C$) format. "$Y$" represents the indoor air temperature (°C) of the insulated model house whereas X_1 is the environment temperature (°C), X_2 is the time (24-h format) (h), and X_3 symbolizes the environment relative humidity (%). The coefficients (m_1, m_2, m_3, C) are obtained from the training data set (through R-Studio).

It should be noteworthy that we did not consider the model without insulation for regression analysis. Because the non-insulated properties are available in most related work. The authors' main intention is to develop a model that predicts the temperature with insulation. Such an equation can be improved through future studies.

Uncertainty analysis

Error analysis was performed to evaluate the performance of statistical models. Based on recommendations provided by Ebtehaj et al. (2015), four indices were proposed for error calculation. Equation (2) to (5) represent mathematical formulation to calculate those indices. All indices were quantified during both training and validation sequence to confirm the consistency of the regression model. How well predictions fit experimental data was determined by the coefficient of determination (R^2) and linearity among predictions and experimental values were determined by Pearson correlation coefficient (R). Both indices being closer to 1 explicate a strong relationship in the model. Further, MAE quantifies absolute residual and RMSE determines the standard deviation of the error component.

$$R^2 = \frac{\sum_{i=1}^{N}(T_P - \overline{T}_E)^2}{\sum_{i=1}^{N}(T_E - \overline{T}_E)^2} = \frac{\text{ModelSum of Squares}}{\text{Total Sum of Squares}}, \quad (2)$$

$$R = \frac{N\sum_{i=1}^{N}(T_P \bullet T_E) - (\sum_{i=1}^{N} T_P \bullet \sum_{i=1}^{N} T_E)}{\sqrt{(N\sum_{i=1}^{N} {T_E}^2 - (\sum_{i=1}^{N} T_E)^2)} \bullet \sqrt{N\sum_{i=1}^{N} {T_P}^2 - (\sum_{i=1}^{N} T_P)^2)}}, \quad (3)$$

$$\text{MAE} = \frac{\sum_{i=1}^{N}|T_P - T_E|}{N}, \quad (4)$$

$$\text{RMSE} = \sqrt{\frac{\sum_{i=1}^{N}(T_P - T_E)^2}{N}}. \quad (5)$$

'T' represents indoor air temperature whereas subscripts 'P' and 'E' denote predicted and experimental values, respectively. $\overline{T}_E$ refers to the mean value of the parent data set, and N refers to the total number of readings.

Cost analysis

The reduction in heat transmittance during the daytime is vital to lower operational energy consumption. Here, the effectiveness of insulation is assessed in terms of two aspects. Foremost, reduction in cooling load is estimated to determine associated cost savings. To calculate energy requirement, an equivalent British thermal unit (BTU) required to cool house was calculated. Several assumptions are hold for calculation: (a) Desired average air temperature = 25 °C; (b) Price of energy 1 Wh = Rs. 0.03; (c) A/C is operated from 6.00 a.m.–6.00 p.m; (d) Variance of outdoor conditions in radiation, humidity, and the wind was not considered. The energy consumption of three model houses and the corresponding cost reduction have been calculated.

CO_2 emission analysis

Accordingly, a reduction in operational energy quantity will decelerate the emission of CO_2. To measure the reduction of CO_2, a carbon calculator of the environment agency was used (Powell, 2011). According to the carbon calculator, 1 kWh of energy consumption is equal to 0.0005937 tCO_2 emissions. The reduction of CO_2 emission due to passive modifications has been calculated accordingly.

Results and discussion

Calculation of thermal conductivity for sawdust and cement insulation

Thermal conductivity of cement grout = 0.80–0.87 W/m K (Kim et al., 2016).

Thermal conductivity of sawdust = 0.038–0.050 W/m K (refer to Table 1).

The arithmetic average was taken for calculations of thermal conductivity.

$$\frac{1}{K_1} = \frac{1-\infty}{K_{ps}} + \frac{\infty}{K_{conc}} = \frac{1-25\%}{0.044} + \frac{25\%}{0.835} = 20.04,$$

$K_1 = 0.058$ W/m K.

Temperature variation on sunny sky condition

Analysis of indoor air temperature

Figure 2 depicts indoor air temperature variation in sunny sky conditions. Proposed insulation lowers the magnitude of peak temperature observed in M1. Further, the temperature variation of M1 consists of disrupted temperature variation. The disrupt changes become moderately consistent for the model with sawdust insulation and RR insulation.

Less pronounced effects of insulated model houses (M2, M3) were appeared between 6–8 h and 16–18 h, compared to the base model. Above variations may be present due to the minimum solar radiation exposure (Handara et al., 2016) on the houses (M2). Even though sawdust–cement insulation (M3) has low thermal conductivity (0.058 W/m K), environment temperature was comparatively lower during the above timeline resulting in minimum temperature variation.

From 11 to 16 h, a slight reduction in indoor air temperature was observed in presence of both insulations. Nevertheless, the decrease in temperature was greater than 1 °C for most of the time. The maximum decrease between M3 and M1 occurred at 12 h. Handara et al. (2016) reported similar observations as a result of intense solar radiation in tropical countries. Simultaneously, the higher solar reflecting ability of RR tape results in a lower air temperature value in the model house (M3). The peak value of M3 was shown at 15 h and it was 33.6 °C, whereas M1 showed a peak value of 35.4 °C. Even though the environmental temperature

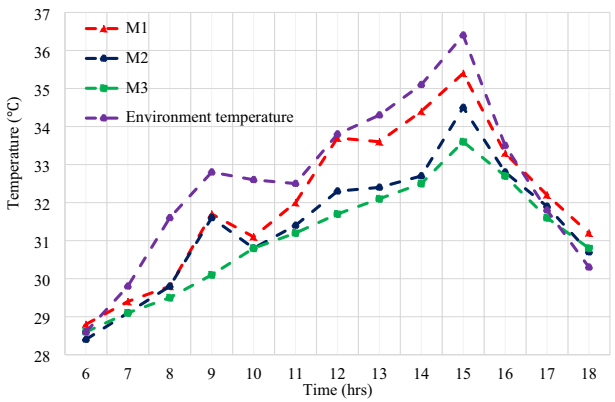

Fig. 2 Indoor air temperature of three models in sunny sky condition

(36.4 °C) was high, the solar intensity was low (Handara et al., 2016) at 12 h. In consequence, the indoor air temperature of M3 has increased. M3 model has recorded lower values of indoor air temperature compared to M2.

These observations show that solar radiation is one of the main causes of adverse thermal conditions. In contrast, it reveals the effectiveness of RR material in improving the thermal environment. However, effects are notable at outer temperatures > 30 °C. Accordingly, materials with higher solar reflectance are appropriate for tropical climates during sunny climatic conditions.

Temperature variation of exterior surface of walls

Generally, the radiant temperature of outer surfaces is an important parameter that affects the thermal performance of a house besides indoor air temperature. Figure 3 depicts exterior surface temperature in M1, M2, and M3 during the test period. A comparable variation in all three model houses is shown in Fig. 3. Lower solar intensity results in a decrease in outer surface temperature for all three models (Handara et al., 2016). As a result of solar reflectance occurring on the surface of RR tape (solar radiation received + solar radiance reflected), the exterior surface temperature of the M3 model becomes gradually higher compared to the other two model houses. However, it did not adversely affect indoor air temperature (Fig. 2) readings and inner surface temperature readings (Fig. 5).

The authors suppose, as a result of solar reflectance occurring on the surface of RR tape (solar radiation received + solar radiance reflected), the exterior surface temperature of the M3 model becomes gradually higher compared to the other two model houses. The contribution of RR material can be observed in the indoor air temperature graphs (Fig. 2), whereas the model that was constructed with RR material showed a lower temperature value compared to the other two model houses.

The direction of solar radiation changes with time due to the rotation of Earth. Hence, global peak values of M3 change from one direction to another. For instance, in the East direction graph (Fig. 3b), M3 showed global peak value (44 °C) at 11 h, and M1 showed global peak value (39 °C) at 15 h. In the North direction (Fig. 3a), M3 showed global peak value (42 °C) at 11 h, and M1 showed global peak value (40 °C) at 15 h. In the South direction (Fig. 3c), M3 showed global peak value (39 °C) at 12 h, and M1 showed global peak value (38 °C) at 15 h. However, in the West direction, M3 (38 °C) showed lower surface temperature compared to M1 (42 °C), and M2 (41 °C).

Effects of shadow (Fig. 4) affect more often on the West side of the wall in the M3 model. It is the reason for the decrease in surface temperature (Fig. 3d) readings of M3 in the West direction. The maximum air temperature (Fig. 2) of

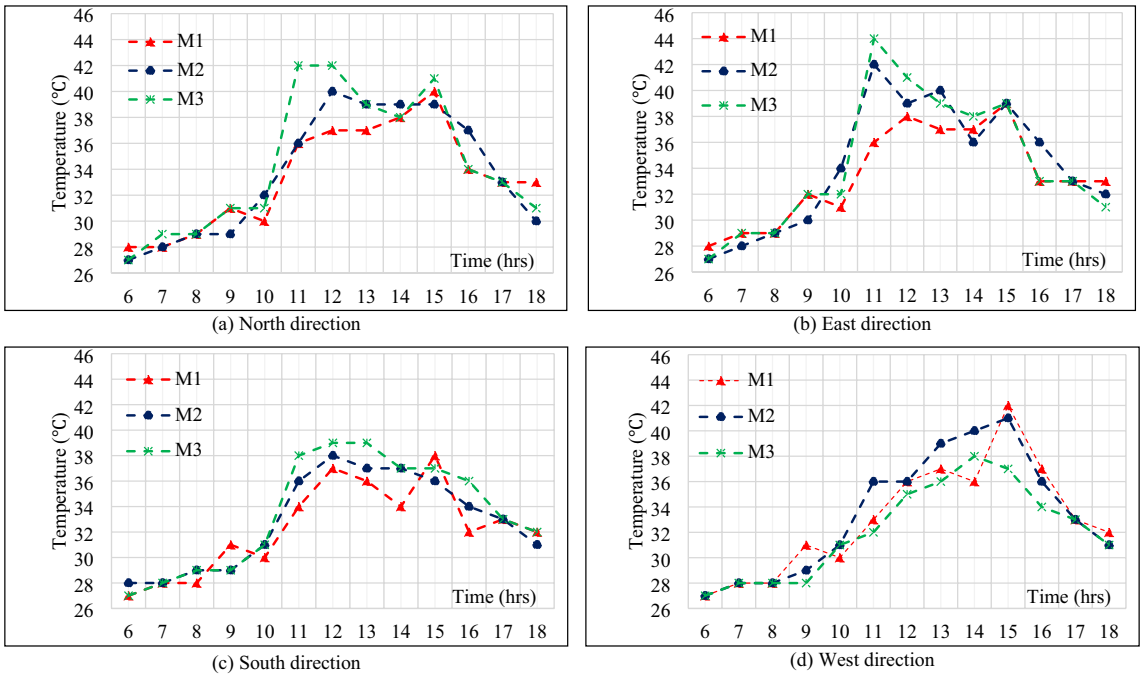

Fig. 3 Outer surface temperature in external walls during sunny sky condition

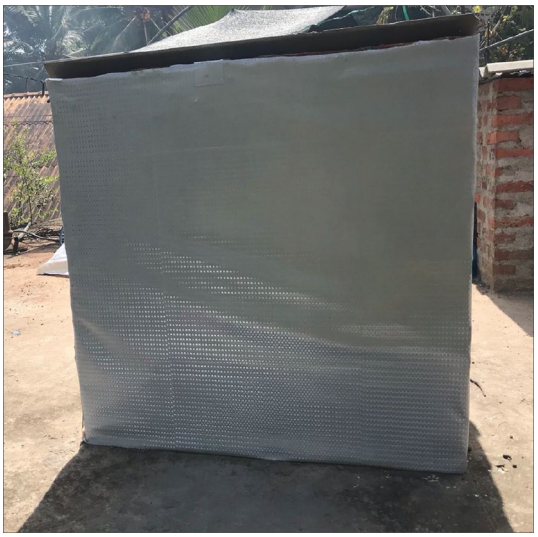

Fig. 4 Shadow (own) in West direction wall in RR model

M1 was observed at 15 h. Similarly, the maximum surface temperature in all four directions for M1 was observed at 15 h.

According to Madrid et al. (2018), sawdust impedes thermal transmittance. Hence, solar radiation will accumulate in outer surface walls. Therefore, exterior surface temperature (M2) has increased in contrast to M1. There was no insulation in M1 to impede the flow of heat from the external to the interior surface. In the North direction (Fig. 3a), the M2 model showed a global peak value (40 °C) at 12 h. In the East direction (Fig. 3b), M2 showed a global peak of (42 °C) at 11 h. A slight increase in temperature was shown from 6 to 10 h in outer surface walls (Fig. 3) and a rapid decrease was observed from 15 to 18 h. Nevertheless, M3 showed maximum global peak value in North (Fig. 3a), East (Fig. 3b), and South direction (Fig. 3c), whereas M1 showed it in West direction (Fig. 3d). From these observations, North, East, and South surfaces are most appropriate to apply RR tape.

Temperature variation of interior surface of walls

Figure 5 depicts inner surface variation for each model. M3 frequently showed a moderate decrease in surface temperature values compared to M2, M1. In addition, temperature readings of M3 in each direction showed rapid growth from 9 to 15 h. For example, the North direction (Fig. 5a) showed a 5 °C increase whereas a 4 °C rise in temperature was observed in the East direction (Fig. 5b). Further, M3 showed a 4 and 6 °C rise, and the South and West direction showed a rise, respectively (Fig. 5c, d). Subsequently, M2 and M1 also showed increased surface temperatures from 9 to 15 h. Nonetheless, M3 showed a more linear temperature increment while the other two models showed moderately disrupt temperature variations. Though the outer surface temperature of M3 has increased up to 38–44 °C (Fig. 3), the inner temperature was in the range of 32–34 °C (Fig. 5). Besides, inner surface temperature readings of M2 were in the range

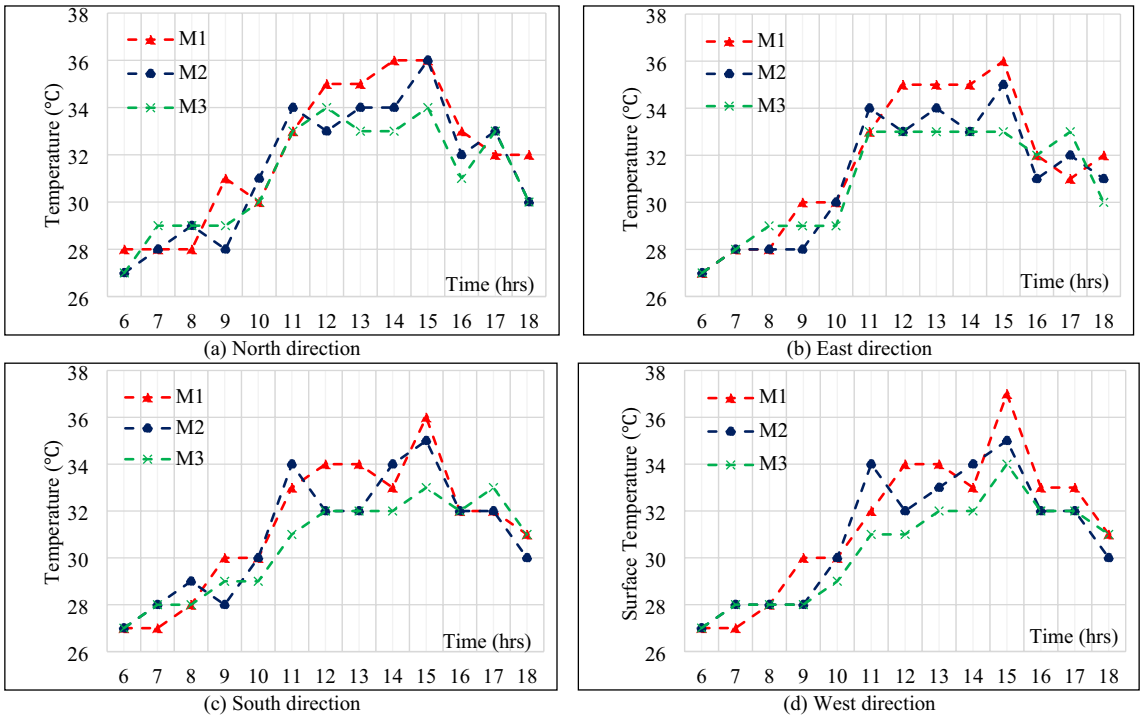

Fig. 5 Inner surface temperature in internal walls during sunny sky condition

of 35–36 °C. Therefore, it convinces the heat accumulation ability of sawdust and the reflective ability of RR material. As a result of the decrease in interior surface temperature, indoor air temperature (Fig. 2) of M3 showed a comparable reduction with respect to the remaining models.

Markedly different temperature variations were not observed for models during the period of 6–9 h. Nonetheless, a significant decrease in temperature was observed from 15 to 18 h. In the North face (Fig. 5a), M3 showed a global peak value (34 °C) at 12 h. Subsequently, M1 showed a global peak value (36 °C) at 15 h. The M2 model showed a global peak value (36 °C) at the same time (15 h) as M1 (36 °C). In the East face (Fig. 5b), a 4-h time lag was observed in the M3 model compared to the M1 model. South (Fig. 5c) and West sides (Fig. 5d) did not show a time lag for the global peak.

Temperature variation in overcast sky conditions

Analysis of indoor air temperature

Indoor air temperature variation in overcast sky conditions is illustrated in Fig. 6. The authors did not conduct experiments during rainy occasions.

The RR insulation cannot alter peak indoor air temperatures compared to the base model (M1) in gloomy weather conditions. Besides, the temperature variation of all models is uniform from 8 to 10 h. M1 and M2 showed a distorted

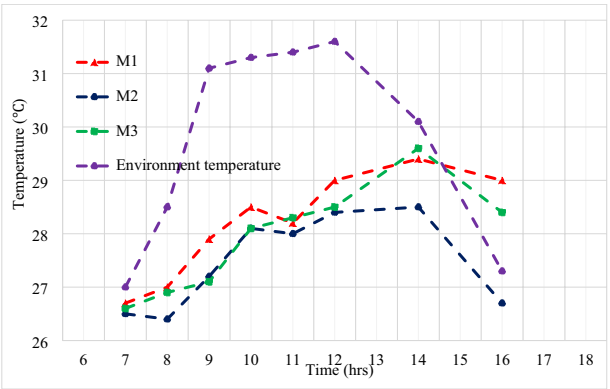

Fig. 6 Air temperature analysis of three models in overcast sky conditions

temperature variation from 11 h. However, both M1 and M2 reach a local peak at 10 h. Still, the maximum decrease in temperature between M2 and M1 occurred at 16 h with a value of 2.3 °C. Further, the M3 model did not show a considerable improvement in indoor air temperature readings.

The model M2 showed the most notable effects during overcast climatic conditions. Sawdust–cement insulation has a lower thermal conductivity (0.058 W/m K) and a higher specific heat capacity (1900–2100 J/kg K—Schiavoni et al., 2016). It shows that the M2 model is a good insulation for tropical countries like Sri Lanka during overcast climatic conditions. However, less heat transmittance has contributed

to lower temperature values (27–30 °C) for the M2 model. Under gloomy weather conditions, the performance of RR tape was reduced as it decreases indoor air temperature by reflecting solar radiation and thermal waves (Castellani et al., 2020; Manni et al. 2018). From the analysis, the authors highlight that RR's performance is strongly dependent on solar radiation and it would be effective for tropical countries. On other hand, sawdust and cement insulation showed effective results for overcast climatic conditions.

Temperature variation of exterior surface of walls

The outer surface temperature of walls in each direction (Fig. 7) shows a comparable variation for all three models. M3 model showed the maximum surface temperature in all four directions and, those were obtained before the rain started (12 h). A considerable decrease in temperature is noticed in all three models after rainy climate conditions (14–16 h). Especially, M3 has decreased about 5 –6 °C in outer surface temperature during this time and M2 decreased about 2–4 °C.

Temperature variation of interior surface of walls

Inner surface temperatures of all three models are shown in Fig. 8. It shows a comparable variation. For example, in the North direction (Fig. 8a) M3 showed the highest surface temperature. Global peak temperatures for all three model houses are observed at 12 h in each direction and with no time lags. M3 model house has recorded the maximum inner surface temperature (34 °C) in the East direction (Fig. 8b). However, a substantial decrease in temperature was observed from 12 to 16 h. For example, M3 showed 3–6 °C difference in temperatures whereas it is 1–3 °C for M2.

Developing a mathematical model to predict indoor air temperature

Regression model for sawdust and cement grout insulation (M2)

$$Y = 0.205X_1 + 0.183X_2 - 0.061X_3 + 26.350$$

Table 2 shows the training and testing phases of the equation developed for the M2 model. During the training sequence, the linear ridge model reached $R = 0.94$ which explains a good linear relationship between independent and dependent parameters. The corresponding R^2 is 0.89 and MAE reached 0.43. The minimum RMSE value of 0.56 was obtained during the training process.

Interestingly, a good agreement existed between each variable, especially during the validation process. The Pearson correlation coefficient (R) has reached 0.93 and MAE has increased up to 0.66. Both R and R^2 describe a good, generalized model despite slight differences in MAE and RMSE values. Figure 9 depicts the correlation between whole predictions and

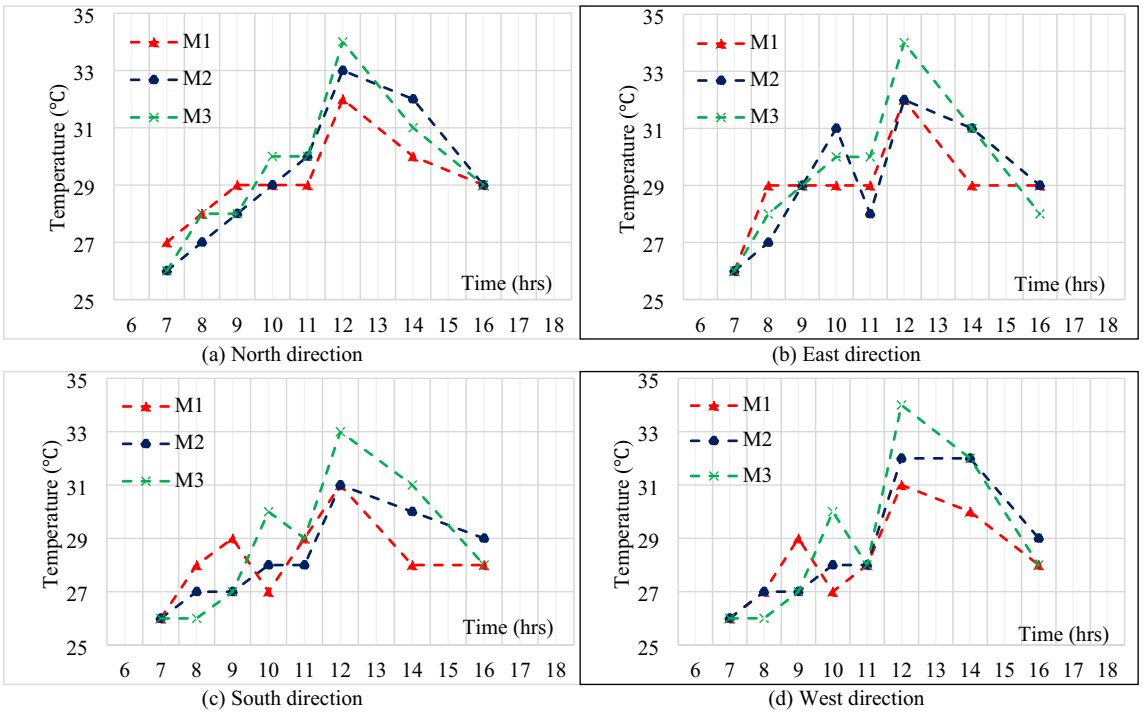

Fig. 7 Outer surface temperature in external walls during overcast sky condition

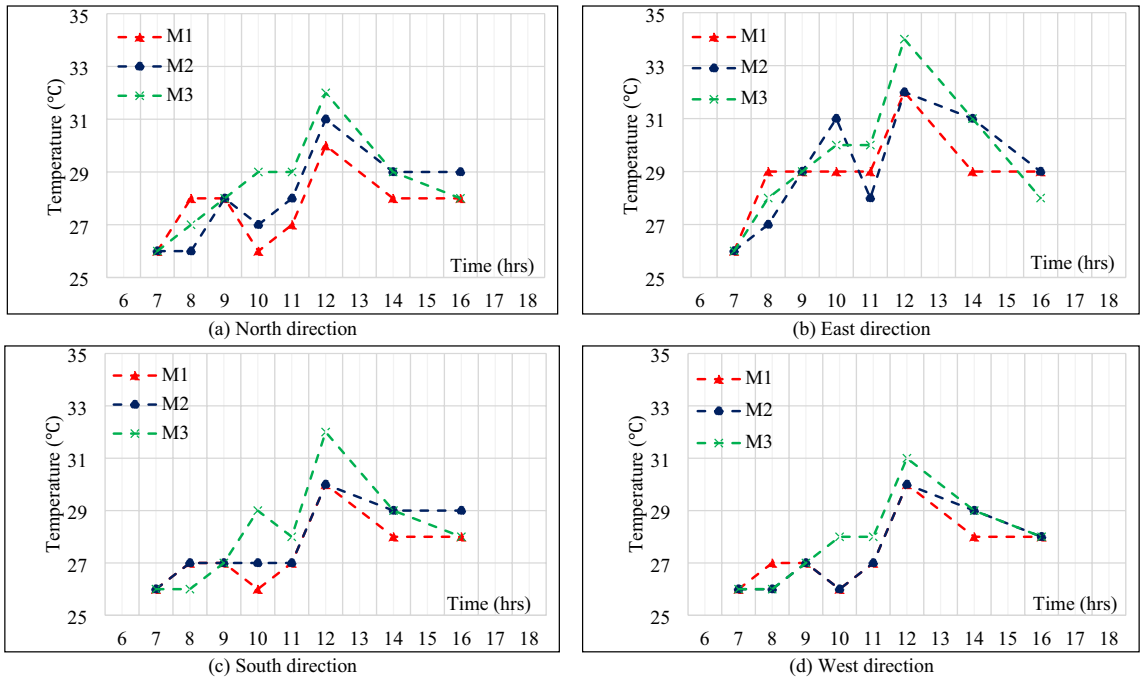

Fig. 8 Inner surface temperature in internal walls during overcast sky condition

Table 2 Performance of regression model for M2 model

	The linear ridge regression model	
Phase	Training	Validation
Correlation (R)	0.94	0.93
Determination (R^2)	0.89	0.87
MAE	0.43	0.66
RMSE	0.56	0.73

Table 3 Performance of regression model for M3 model

Indices	The linear ridge regression model	
Phase	Training	Validation
Correlation (R)	0.78	0.96
Determination (R^2)	0.61	0.92
MAE	1.11	0.32
RMSE	1.53	0.44

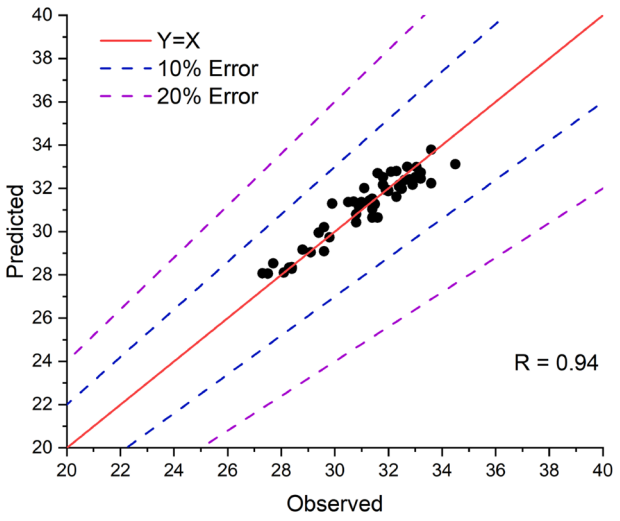

Fig. 9 Comparison of indoor air temperature calculated from (M2) regression model with experimental results (Red line represents $x=y$ line)

experimental data (scale has been enlarged for a clear representation of results). It appeared all predictions lie well within the 10% error limit. For instance, R reached 0.94 for the whole prediction, confirming the validity of the statistical model. These models were developed primarily based on clay brick with an overall wall thickness of 0.225 m (including plaster thickness of 0.025 m) and a floor area of 0.25 m^2. Nevertheless, it does not rule out these equations to be modified with various walling materials and floor areas. However, such an attempt should be given after following a thorough series of experimental work.

Regression model for RR insulation (M3)

$$Y = 0.244X_1 + 0.086X_2 - 0.096X_3 + 28.791$$

Table 3 explained, for the model with RR insulation, training accuracy reached an R of 0.78. This shows a considerable reduction compared to the training phase of the M2 model. We note that the data set consists of some inconsistencies such that the

model will be moderately generalized. Thus, MAE and RMSE at the training process reached 1.11 and 1.53 which are higher compared to the values obtained for the M2 model (MAE = 0.47 and RMSE = 0.56). However, the validation process ended up with $R = 0.96$ which is an acceptable limit for predictions. Fascinatingly, MAE and RMSE have decreased in contrast to computed values for the M2 model. Repeatedly, this equation is valid only for insulation with clay brick with a wall thickness of 0.2 m. Overall predictions are shown in Fig. 10 (scale has been enlarged for a clear representation of results). It has obtained an *R*-value of 0.8, convincing a good agreement between the experiment and statistical model. Figure 10 shows that are several instances where prediction deviates beyond 10% with respect to limit. Plausibly, ridge regression provides a fair and non-complicated statistical model for each scenario. However, corresponding predictions of both equations did not exceed 20% error.

Estimation of energy in model houses

- Area of the model House = $0.9 \times 0.9 = 0.81$ m^2.
- Wall thickness = 0.20 m.
- Floor area of the model house = $0.5 \times 0.5 = 0.25$ m^2 (Fig. 11).
- Model house height = 0.9 m.

The plan view of the constructed model house is shown in Fig. 11 and the energy requirement (BTU) for each model house is calculated in Table 4.

Energy cost estimation for model houses

Energy consumed by the A/C (M2) = 1318×0.293 Wh = 386.17 Wh.

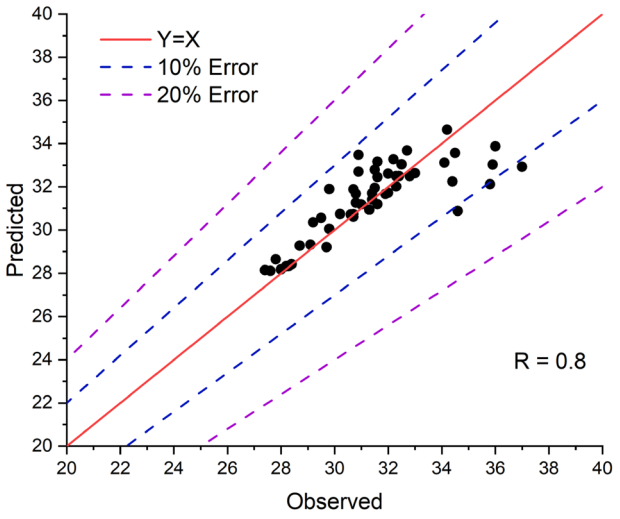

Fig. 10 Comparison of indoor air temperature calculated from (M3) regression model with experimental results (Red line represents $x = y$ line)

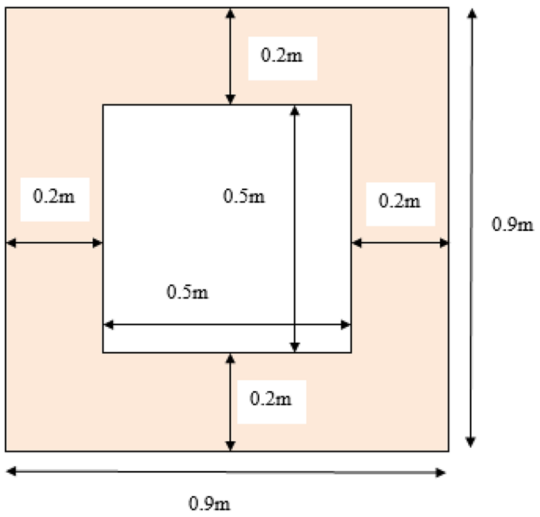

Fig. 11 Plan view of the model house

Energy consumed by the A/C per m^2 (M2) = $\frac{386.17\text{Wh}}{0.5\times0.5\text{m2}} = 1544.68$ Wh.

Cost of energy per day (M2) = 386.17 Wh × Rs. 0.03/Wh = Rs.11.59.

Cost of energy per month (M2) = Rs. 11.59/day × 30 days = Rs. 347.70.

Cost of energy per year (M2) = Rs. 347.70/month × 12 months = Rs. 4172.40.

Cost of energy in a year per m^2 (M2) = $\frac{\text{Rs.4172.40/year}}{0.5\times0.5\text{m2}}$ = Rs. 16,689.60.

Cost of energy per year (M1) = Rs. 382.2/month × 12 months = Rs. 4586.40.

Cost of energy in a year per m^2 (M1) = $\frac{\text{Rs.4586.40/year}}{0.5\times0.5\text{m2}}$ = Rs. 18,345.60.

% Cost of energy reduced with modifications (M2) = $\frac{\text{Rs.18345.60}-\text{Rs.16689.60}}{\text{Rs.18345.60}} \times 100\% = 9.03\%$.

In the USA, commercial buildings use 17.6 quadrillions of BTU'S and it is anticipated to increase by another 3.3 quadrillions BTUs from 2012 to 2040 (Biswas et al., 2016). Table 5 shows the contribution of insulation materials for reducing cost due to energy by decreasing BTU demand in terms of air conditioning. We obtained a 9% reduction in energy cost in the M2 model compared to the M1 model and the corresponding reduction is around 13% for the model with RR insulation.

Emission level estimation for model houses

tCO_2 emission per day (M2) = $0.0005937 \times 0.38617 = 0.00$ 02293.

tCO_2 emission per month (M2) = 0.0002293/day × 30 days = 0.006878.

tCO_2 emission per year (M2) = 0.006878/month × 12 months = 0.08254.

Table 4 Calculation of energy requirement for model houses

Time (h)	Name of the model house											
	M1				M2				M3			
	Inside temperature (°C)	Temperature desired (°C)	Temperature change (°C)	Equivalent BTU (Calculator, 2021)	Inside temperature (°C)	Temperature desired (°C)	Temperature change (°C)	Equivalent BTU (Calculator, 2021)	Inside temperature (°C)	Temperature desired (°C)	Temperature change (°C)	Equivalent BTU (Calculator, 2021)
6	28.8	25	3.8	60	28.4	25	3.4	54	28.6	25	3.6	57
7	29.4	25	4.4	69	29.1	25	4.1	65	29.1	25	4.1	65
8	29.8	25	4.8	76	29.8	25	4.8	76	29.5	25	4.5	71
9	31.7	25	6.7	106	31.6	25	6.6	104	30.1	25	5.1	81
10	31.1	25	6.1	96	30.8	25	5.8	92	30.8	25	5.8	92
11	32	25	7	111	31.4	25	6.4	101	31.2	25	6.2	98
12	33.7	25	8.7	138	32.3	25	7.3	115	31.7	25	6.7	106
13	33.6	25	8.6	136	32.4	25	7.4	117	32.1	25	7.1	112
14	34.4	25	9.4	149	32.7	25	7.7	122	32.5	25	7.5	119
15	35.4	25	10.4	165	34.5	25	9.5	150	33.6	25	8.6	136
16	33.3	25	8.3	131	32.8	25	7.8	123	32.7	25	7.7	122
17	32.2	25	7.2	114	31.9	25	6.9	109	31.6	25	6.6	104
18	31.2	25	6.2	98	30.7	25	5.7	90	30.8	25	5.8	92
Sum of the BTU				∑1449				∑1318				∑1255

Table 5 Energy cost analysis of physical models

Calculation of energy and cost for electricity in model houses	Model house name		
	M1	M2	M3
BTU required to cool the model house per day (BTU)	1449	1318	1255
1 BTU = 0.293Wh (conversion factor for BTU)			
Energy consumed by the A/C (Wh)	424.56	386.17	367.72
Energy consumed by the A/C (Wh) per m^2	1698.24	1544.68	1470.88
The cost of energy per unit is Rs. 0.03/Wh			
Cost of energy per day (Rs.)	12.74	11.59	11.03
Cost of energy per month (Rs.)	382.2	347.70	330.90
Cost of energy per year (Rs.)	4586.40	4172.40	3970.80
Cost of energy in a year per m^2 (Rs.)	18,345.60	16,689.60	15,883.20
% Cost of energy reduced with modifications	–	9.03%	13.4%

Table 6 Calculation of CO_2 emission

Model house name	M1	M2	M3
The emission of tCO_2 per kWh is 0.0005937 (Powell, 2011)			
Energy consumed by A/C (Wh)	424.56	386.17	367.72
Energy consumed by A/C (kWh)	0.42456	0.38617	0.36772
tCO_2 emission per day	0.0002521	0.0002293	0.0002183
tCO_2 emission per month	0.007562	0.006878	0.006549
tCO_2 emission per year	0.09070	0.08254	0.07859
1 ton = 907.185 kg (conversion factor for ton)			
$kgCO_2$ emission per year	82.28	74.88	71.30
$kgCO_2$ emission per m^2 in a year	329.12	299.52	285.20
$kgCO_2$ reduced	–	29.6	43.92
% of CO_2 emission reduced due to modifications	–	9%	13.3%

$kgCO_2$ emission per year (M2) = $0.08254 \times 907.185 = 74.88$.

$kgCO_2$ emission per m^2 in a year (M2) = $\frac{74.88}{0.5 \times 0.5} = 299.52$.

$kgCO_2$ reduced (M2) = $329.12 - 299.52 = 29.6$.

% Of CO_2 emission due to modifications (M2) = $\frac{329.12-299.52}{329.12} \times 100\% = 9\%$.

Table 6 shows the contribution of insulation materials for reducing CO_2 emission levels. A 9% reduction of CO_2 emission levels was obtained for the M2 model compared to the M1 model and the corresponding reduction is around 13% for the model with RR insulation. When emission levels are considered, each insulation provides similar percentages for energy cost reduction. These calculations were performed considering small model scale conditions. Therefore, it stresses that these values will become significant on a real scale. Many researchers have already described the importance of reducing CO_2 content worldwide. Tettey et al. (2014) reported that one-third of global greenhouse gas emissions are due to building's energy consumption. Proper control in energy utilization is a must to reduce greenhouse emissions (Rosas-Flores & Rosas-Flores, 2020). It recommends community employ passive features in design stages rather than active measures during the operational stage. It likewise elucidates the possibility of passive features to enhance the energy efficiency of envelope components. Generally, with tropical climatic conditions, individual heated envelopes can create urban heat islands. Despite high energy demand, such heat islands drastically increase the surrounding temperature. Therefore, it is essential to address these aspects at the design stage of a building.

Conclusions

This study has addressed the lack of design aspects to improve the energy efficiency of buildings using alternative materials including waste materials. In this study, wall insulation methods were developed using sawdust and retro-reflective materials. Sawdust is considered to be a waste material in the carpentry industry and retro-reflective contains good reflective characteristics.

- Overall, models with insulations provide a significant temperature reduction in the indoor surface and a fair reduction in indoor air temperature. The model house with sawdust–cement mortar resulted in a 9% reduction in carbon emissions whereas it is 13% for the model with retro-reflective material.
- Further, regression models developed on experimental results showed a good agreement ($R > 0.8$). The authors recommend linear ridge regression models to predict indoor air temperature with different insulation materials.

Plausibly, this study stresses the importance of utilizing sawdust and retro-reflective materials to improve the thermal environment inside a building, reducing associated daytime operational energy demand.

Limitations of the study

The present study was focused on small-scale model houses to investigate the thermal performance of sawdust and retro-reflective materials.

- However, the effect of this insulation should be further investigated on a real scale model. As well as, the long-term performance of insulated models must be given attention. To confirm these results and improve the study further, the following measures are recommended (e.g., temperature, wind speed, humidity. solar radiation intensity, building ventilation).
- Energy modeling would be an appropriate solution to investigate the effect of insulation on a real scale with both latent and sensible heat components. Moreover, limited experimental conditions were available whereas it was difficult to simulate different orientations, the effect of passive features. Energy modeling provides sophisticated analysis options at any stage of a construction (e.g., construction stage, operational stage, etc.). For instance, analytical modeling will be supportive to determine the optimum thickness of insulation to be utilized in tropical climatic conditions.
- We recommend this study to conduct in a country other than the tropical context. Because the actual effect of insulation in both warm and cold climates should be evaluated. A markedly different seasonal variation will strongly affect the annual energy consumption. Further, the study used unique insulation for each model. However, the results do not rule out the possibility of combining insulations for a specific model. That may improve the desired thermal conditions inside a house.

Annexure

Annex 01: Cost for different model houses

The construction cost for each model house was calculated. All prices are in Sri Lankan Rupees (LKR). size of the house is $0.9 \times 0.9 \times 0.9$ m with an opening of 0.3×0.3 m. size of asbestos sheets was 1×1 m and the size of standard engineering bricks was $0.195 \times 0.090 \times 0.055$ m.

Item no	Material	Unit price (LKR)	Quantity	Price (LKR)
01	Bricks	12.50	350 bricks	4375.00
02	Cement bags	950.00	0.8 bags	760.00
03	Sand	16,000.00	0.15 cube	2400.00
04	Asbestos sheet	2975.00	1/3	991.67
05	Mason	3000.00	0.7 days	2100.00
Total price (LKR)				10,626.67

Annex 02: Cost for the model with RR insulation

Item no	Material	Unit price (LKR)	Quantity	Price (LKR)
01	Bricks	12.50	350 bricks	4375.00
02	Cement bags	950.00	0.8 bags	760.00
03	Sand	16,000.00	0.15 cube	2400.00
04	Asbestos sheet	2975.00	1/3	991.67
06	Diamond cut RR tape (white color)	430.00	9 ft^2	3870.00
05	Mason	3000.00	0.7 days	2100.00
Total price (LKR)				14,496.67

Annex 03: Cost for the model with sawdust insulation

Item no	Material	Unit price (LKR)	Quantity	Price (LKR)
01	Bricks	12.50	350 bricks	4375.00
02	Cement bags	950.00	1.55 bags	1472.50
03	Sand	16,000.00	0.15 cube	2400.00
04	Asbestos sheet	2975.00	1/3	991.67
05	Saw dust	30.00	5 kg	150.00
06	Mason	3000.00	1.3 days	3900.00
Total price (LKR)				13,290.00

Annex 04: Solar radiation graphs

Solar radiation graphs for Colombo Sri Lanka were taken using the Metenorm application.

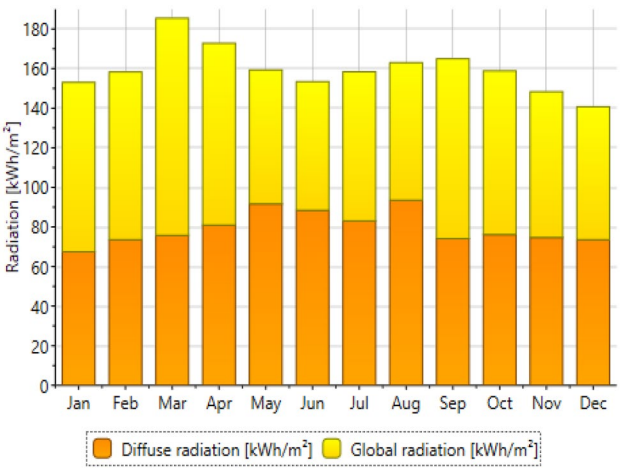

Solar radiation graph for Colombo

Annex 05: Thermal properties of various materials and their application

Name of material	Thermal conductivity (W/m K)	Thermal resistance (m^2K/W)	Thermal diffusivity (m^2/s) $\times 10^{-6}$	Specific heat capacity (J/kg K)	Solar reflectance (albedo value)	Density (kg/m^3)	Possible ways to use in a model house (insulation)
Fiber glass (recycled)	0.031 (Schiavoni et al., 2016)			830 (Schiavoni et al., 2016)		450 (Schiavoni et al., 2016)	Fix in windows
Foam glass	0.04 (Braulio-Gonzalo & Bovea, 2017)			1000 (Braulio-Gonzalo & Bovea, 2017)		110 (Braulio-Gonzalo & Bovea, 2017)	Fix in windows
Stone wool	0.033–0.040 (Karamanos, et al., 2008)			800–1000 (Schiavoni et al., 2016)		40–200 (Karamanos, et al., 2008)	Insulate in internal walls
Cellulose	0.037–0.042 (Schiavoni et al., 2016)			1300–1600 (Schiavoni et al., 2016)		30–80 (Schiavoni et al., 2016)	Insulate in internal walls by blown or damp sprayed
Polyurethane foam (PIR)	0.0236 (Biswas et al., 2016)			1300–1450 (Schiavoni et al., 2016)		29 (Biswas et al., 2016)	Insulate between walls
Expanded polystyrene (EPS)	0.041 (Meng et al., 2018)			1280 (Meng et al., 2018)		22 (Meng et al., 2018)	Insulate between walls
Silica aerogel	1.010–0.030 (Casini, 2016)			1000 (Schiavoni et al., 2016)		5–200 (Casini, 2016)	Sandwiched within double glazed window units
Concrete block	0.435 (Alausa et al., 2013)	2.299 (Alausa et al., 2013)	1.022 (Alausa et al., 2013)			2100–2300 (Grabarz et al., 2012)	Construct model house structure
Laterite mud	0.523 (Alausa et al., 2013)	1.912 (Alausa et al., 2013)	1.126 (Alausa et al., 2013)				Construct model house structure
Cement mortar	0.840 (Meng et al., 2018)			840 (Meng et al., 2018)		1860 (Meng et al., 2018)	Apply between two bricks or blocks as a binding agent
Silicate blocks (0.25 m)	0.41 (Dudzińska & Kotowicz, 2015)			880 (Dudzińska & Kotowicz, 2015)		1400 (Dudzińska & Kotowicz, 2015)	Construct model house structure
Cellular concrete blocks	0.17 (Dudzińska & Kotowicz, 2015)			840 (Dudzińska & Kotowicz, 2015)		600 (Dudzińska & Kotowicz, 2015)	Construct model house structure
Solid brick	0.77 (Dudzińska & Kotowicz, 2015)			880 (Dudzińska & Kotowicz, 2015)		1800 (Grabarz et al., 2012)	Construct model house structure
Rock wool	0.04 (Rosas-Flores & Rosas-Flores, 2020)					50–80 (Đurović-Petrović, 2015)	Insulate in ceiling
Cork	0.045 (Barrau et al., 2014)			1500–1700 (Schiavoni et al., 2016)		110–170 (Schiavoni et al., 2016)	Insulate in ceiling

Name of material	Thermal conductivity (W/m K)	Thermal resistance (m^2K/W)	Thermal diffusivity (m^2/s) $\times 10^{-6}$	Specific heat capacity (J/kg K)	Solar reflectance (albedo value)	Density (kg/m^3)	Possible ways to use in a model house (insulation)
Sawdust	0.038–0.050 (Schiavoni et al., 2016)			1900–2100 (Schiavoni et al., 2016)		50–270 (Schiavoni et al., 2016)	Use as a cement, sawdust composite mixture and apply in the external wall as a plaster
Extruded polystyrene	0.0320 (Biswas et al., 2016)			1450–1700 (Schiavoni et al., 2016)		30 (Biswas et al., 2016)	Insulate in outer or internal walls
Phenolic foam	0.018–0.024 (Schiavoni et al., 2016)			1300–1400 (Schiavoni et al., 2016)		40–160 (Schiavoni et al., 2016)	Insulate in internal walls
Hempcrete (1:1)	0.074–0.103 (Dhakal et al., 2017)					233–388 (Dhakal et al., 2017)	Insulate in external walls
Hemp fiber	0.038–0.060 (Schiavoni et al., 2016)			1600–1700 (Schiavoni et al., 2016)		20–90 (Schiavoni et al., 2016)	Insulate in external walls
Glass wool	0.04 (Rosas-Flores & Rosas-Flores, 2020)			900–1000 (Schiavoni et al., 2016)		15–75 (Schiavoni et al., 2016)	Insulate in ceiling
Sheep wool	0.038–0.054 (Schiavoni et al., 2016)			1300–1700 (Schiavoni et al., 2016)		10–25 (Schiavoni et al., 2016)	Insulate in internal walls
Recycled cotton	0.039–0.044 (Schiavoni et al., 2016)			1600 (Schiavoni et al., 2016)		25–45 (Schiavoni et al., 2016)	Apply between walls
Straw bale	0.052–0.06 (Costes et al., 2017)			600 (Schiavoni et al., 2016)		75–90 (Costes et al., 2017)	Insulate in internal walls
Rice hulls	0.046–0.566 (Yarbrough et al., 2005)					154–168 (Yarbrough et al., 2005)	Insulate in external walls
Retro-reflective tape (RR)	2.026 (Meng et al., 2016)			1324 (Meng et al., 2016)	0.81 (Yuan et al., 2015)	307 (Meng et al., 2016)	Insulate in external walls
Clay tile	0.7106 (Ariyadasa et al., 2015)					1790 (Ariyadasa et al., 2015)	Provide as a shading material for model house
Asbestos sheet	0.4733 (Ariyadasa et al., 2015)					1630 (Ariyadasa et al., 2015)	Provide as a shading material for model house
Cement tile	0.5619 (Ariyadasa et al., 2015)					2160 (Ariyadasa et al., 2015)	Provide as a shading material for model house

Acknowledgements Authors like to convey their sincere gratitude to the Sri Lanka Institute of Information Technology for facilitating experiments and research work. Further, we thank the reviewers for their constructive suggestions to improve the quality of the paper.

Funding No funding was recieved to assist with the preparation of this manuscript.

Declarations

Conflict of interest The authors declare that they do not have any conflict of interest.

References

Aditya, L., Mahlia, T. M. I., Rismanchi, B., Hasan, M. H., & Metseelar, H. S. C. (2017). A review on insulation materials for energy conservation in buildings. *Renewable and Sustainable Energy Reviews, 73*, 1352–1365. https://doi.org/10.1016/j.rser.2017.02.034

Alausa, S., Adekoya, B., Aderibigbe, J., & Nwaokocha, C. (2013). Thermal characteristics of laterite-mud and concrete-block for walls in building construction in Nigeria. *International Journal of Engineering and Applied Sciences, 4*(4), 1–4.

Al-Tamimi, A. S., Baghabra Al-Amoudi, O. S., Al-Osta, M. A., Ali, M. R., & Ahmad, A. (2020). Effect of insulation materials and cavity layout on heat transfer of concrete masonry hollow blocks. *Construction and Building Materials, 254*, 119300. https://doi.org/10.1016/j.conbuildmat.2020.119300

Andiç-Çakir, Ö., Son, A. E., Sürmelioğlu, S., Tosun, E., & Sarikanat, M. (2021). Improvement of traditional clay bricks' thermal insulation characteristics by using waste materials. *Case Studies in Construction Materials, 15*, e00560. https://doi.org/10.1016/j.cscm.2021.e00560

Annibaldi, V., Cucchiella, F., Berardinis, P. D., Gastaldi, M., & Rotilio, M. (2019). An integrated sustainable and profitable approach of energy efficiency in heritage buildings. *Journal of Cleaner Production*. https://doi.org/10.1016/j.jclepro.2019.119516

Annibaldi, V., Cucchiella, F., & Rotilio, M. (2021). Economic and environmentalassessment of thermal insulation. A case study in Italian context. *Case Studies in Construction Materials*. https://doi.org/10.1016/j.cscm.2021.e00682

Ariyadasa, G. L. M., Muthurathne, S. S. K., & Adikary, S. U. (2015). Investigating the physical, mechanical and thermal properties of common roofing materials in Sri Lanka. In *Proceedings of 6th annual national building research symposium*, Sri Lanka.

Asdrubali, F., Baldassarri, C., & Fthenakis, V. (2013). Life cycle analysis in construction sector: Guiding optimization of conventional Italian buildings. *Energy and Buildings, 64*, 73–89. https://doi.org/10.1016/j.enbuild.2013.04.018

Barrau, J., Ibañez, M., & Badia, F. (2014). Impact of optimization criteria on determination of insulation thickness. *Energy and Buildings, 76*, 459–469. https://doi.org/10.1016/j.enbuild.2014.03.017

Biswas, K., Shrestha, S. S., Bhandari, M. S., & Desjarlais, A. O. (2016). Insulation materials for commercial buildings in North America: An assessment of lifetime energy and environmental impacts. *Energy and Buildings, 112*, 256–269. https://doi.org/10.1016/j.enbuild.2015.12.013

Braulio-Gonzalo, M., & Bovea, M. D. (2017). Environmental and cost performance of building's envelope insulation materials to reduce energy demand: Thickness optimisation. *Energy and Buildings, 150*, 527–545. https://doi.org/10.1016/j.enbuild.2017.06.005

Calculator, b. (2021). *BTU Calculator*. [online] Calculator.net. Available at: https://www.calculator.net/btu-calculator.html. Accessed 27 October 2020.

Casini, M. (2016). 4—Advanced insulating materials. In M. Casini (Ed.), *Smart buildings* (pp. 127–177). Woodhead Publishing.

Castellani, B., Gambelli, A., Nicolini, A., & Rossi, F. (2020). Optic-energy and visual comfort analysis of retro-reflective building plasters. *Building and Environment, 174*, 106781.

Cetiner, I., & Shea, A. D. (2018). Wood waste as an alternative thermal insulation for buildings. *Energy and Buildings, 168*, 374–384. https://doi.org/10.1016/j.enbuild.2018.03.019

Claudiu, A. (2014). Use of sawdust in composition of plaster mortars. *ProEnvironment, 7*, 30–34.

Costes, J., Evrard, A., Biot, B., Keutgen, G., Daras, A., Dubois, S., Lebeau, F., & Courard, L. (2017). Thermal conductivity of straw bales: full size measurements considering direction of heat flow. *Buildings, 7*(4), 11.

de Dear, R., Akimoto, T., Arens, E., Brager, G., Candido, C., Cheong, K., Li, B., Nishihara, N., Sekhar, S., Tanabe, S., Toftum, J., Zhang, H., & Zhu, Y. (2013). Progress in thermal comfort research over last twenty years. *Indoor Air, 23*(6), 442–461.

Dhakal, U., Berardi, U., Gorgolewski, M., & Richman, R. (2017). Hygrothermal performance of hempcrete for Ontario (Canada) buildings. *Journal of Cleaner Production, 142*, 3655–3664. https://doi.org/10.1016/j.jclepro.2016.10.102

Dissanayake, D. M. K. W., Jayasinghe, C., & Jayasinghe, M. T. R. (2009). A comparative embodied energy analysis of a house with recycled expanded polystyrene (EPS) based foam concrete wall panels. *Energy and Buildings, 135*, 85–94. https://doi.org/10.1016/j.enbuild.2016.11.044

Dudzińska, A., & Kotowicz, A. (2015). Features of materials versus thermal comfort in a passive building. *Procedia Engineering, 108*, 108–115.

Đurović-Petrović, M. (2015). Experimental investigation of rockwool insulation hygrothermal properties related to material structure. *Thermal Science, 19*, 923–928. https://doi.org/10.2298/TSCI131216168D

Ebtehaj, I. H., Bonakdari, H., Zaji, A. H., Azimi, H., & Khoshbin, F. (2015). GMDH-type neural network approach for modeling discharge coefficient of rectangular sharp-crested side weirs. *International Journal of Engineering Science and Technology, 18*(4), 746–757. https://doi.org/10.1016/j.jestch.2015.04.012

Feidt, M. (2018). *Finite physical dimensions optimal thermodynamics 1: Fundamentals* (1st ed., pp. 1–41). Amsterdam: Elsevier.

Gopinath, K., Anuratha, K., Harisundar, R., & Saravanan, M. (2015). Utilization of saw dust in cement mortar & cement concrete. *International Journal of Scientific & Engineering Research (IJSER), 6*(8), 665–682.

Grabarz, R. C., Souza, L. C. L., & Parsekian, G. A. (2012). Theoretical analysis of thermal performance of clay and concrete masonry structural under various conditions. In *15th International brick and block masonry conference*, Florianópolis, Brazil.

Hafed, S. (2017). Study of thermal insulation and some mechanical properties for hybrid composites (cement – wood sawdust). *International Journal of Computation and Applied Sciences IJOCAAS, 3*(2), 212–216.

Haik, R., Peled, A., & Meir, I. A. (2020). Thermal performance of lime hemp concrete (LHC) with alternative binders. *Energy and Buildings, 210*, 109740. https://doi.org/10.1016/j.enbuild.2019.109740

Halwatura, R. (2014). Performance of insulated roofs with elevated outdoor conditions due to global warming. *Journal of Environmental Treatment Techniques, 2*, 134–142.

Halwatura, R. U., & Jayasinghe, M. T. R. (2008). Thermal performance of insulated roof slabs in tropical climates. *Energy and Buildings, 40*(7), 1153–1160. https://doi.org/10.1016/j.enbuild.2007.10.006

Halwatura, R. U., & Jayasinghe, M. T. R. (2009). Influence of insulated roof slabs on air conditioned spaces in tropical climatic conditions—A life cycle cost approach. *Energy and Buildings, 41*, 678–686.

Handara, V., Illya, G., Tippabhotla, S. K., Shivakumar, R., & Budiman, A. (2016). Center for Solar Photovoltaics (CPV) at Surya University: Novel and innovative solar photovoltaics system designs for tropical and near-ocean regions (an overview and research directions). *Procedia Engineering, 139*, 22–31. https://doi.org/10.1016/j.proeng.2015.09.211

James, G., Witten, D., Hastie, T., & Tibshirani, R. (2017). *An introduction to statistical learning* (8th ed., pp. 244–255). Springer.

Karamanos, A., Hadiarakou, S., & Papadopoulos, A. (2008). Impact of temperature and moisture on thermal performance of stone wool. *Energy and Buildings, 40*(8), 1402–1411.

Khoukhi, M. (2018). Combined effect of heat and moisture transfer dependent thermal conductivity of polystyrene insulation material: Impact on building energy performance. *Energy and Buildings, 169*, 228–235. https://doi.org/10.1016/j.enbuild.2018.03.055

Kim, D., Kim, G., & Baek, H. (2016). Thermal conductivities under unsaturated condition and mechanical properties of cement-based grout for vertical ground-heat exchangers in Korea—A case study. *Energy and Buildings, 122*, 34–41. https://doi.org/10.1016/j.enbuild.2016.02.047

Leo Samuel, D., Dharmasastha, K., Shiva Nagendra, S., & Maiya, M. (2017). Thermal comfort in traditional buildings composed of local and modern construction materials. *International Journal of Sustainable Built Environment, 6*(2), 463–475.

Lin, B., & Liu, H. (2015). China's building energy efficiency and urbanization. *Energy and Buildings, 86*, 356–365.

Madrid, M., Orbe, A., Carré, H., & García, Y. (2018). Thermal performance of sawdust and lime-mud concrete masonry units. *Construction and Building Materials, 169*, 113–123.

Mallik, F. H. (1996). Thermal comfort and building designing in tropical climates. *Energy and Buildings, 23*(3), 161–167. https://doi.org/10.1016/0378-7788(95)00940-X

Manni, M., Lobaccaro, G., Goia, F., & Nicolini, A. (2018). An inverse approach to identify selective angular properties of retro-reflective materials for urban heat island mitigation. *Solar Energy, 176*, 194–210. https://doi.org/10.1016/j.solener.2018.10.003

Meddage, D. P. P., & Jayasinghe, M. T. R. (2022). Use of EPS based light-weight concrete panels as a roof insulation material for NERD slab system. In R. Dissanayake, P. Mendis, K. Weerasekera, S. De Silva, & S. Fernando (Eds.), *ICSBE 2020* (pp. 375–384). Springer.

Meng, X., Huang, Y., Cao, Y., Gao, Y., Hou, C., Zhang, L., & Shen, Q. (2018). Optimization of wall thermal insulation characteristics based on intermittent heating operation. *Case Studies in Construction Materials, 9*, e00188. https://doi.org/10.1016/j.cscm.2018.e00188

Meng, X., Luo, T., Wang, Z., Zhang, W., Yan, B., Ouyang, J., & Long, E. (2016). Effect of retro-reflective materials on building indoor temperature conditions and heat flow analysis for walls. *Energy and Buildings, 127*, 488–498.

Meng, X., Wang, C., Liang, W., Wang, S., Li, P., & Long, E. (2015). Thermal performance improvement of prefab houses by covering retro-reflective materials. *Procedia Engineering, 121*, 1001–1007.

Nandapala, K., & Halwatura, R. U. (2016). Design of a durable roof slab insulation system for tropical climatic conditions. *Cogent Engineering, 3*, 1196526.

Oluyamo, S., & Bello, O. (2014). Particle sizes and thermal insulation properties of some selected wood materials for solar device applications. *IOSR Journal of Applied Physics (IOSR-JAP), 6*(2), 54–58.

Powell, A. (2011). *370_07_SD01 Construction carbon calculator,* electronic data set. Environment Agency, viewed 22 November 2020; https://data.gov.uk/data/contracts-finder-archive/download/355422/39ef8800-9ca6-43b3-b893-5b6399cf7374.

Progelhof, R. C., Throne, J. L., & Ruetsch, R. R. (1976). Methods for predicting thermal conductivity of composite systems: A review. *Polymer Engineering & Science, 16*(9), 615–625.

Rosas-Flores, J. A., & Rosas-Flores, D. (2020). Potential energy savings and mitigation of emissions by insulation for residential buildings in Mexico. *Energy and Buildings, 209*, 109698. https://doi.org/10.1016/j.enbuild.2019.109698

Rossi, B., Marique, A.-F., Glaumann, M., & Reiter, S. (2012). Life-cycle assessment of residential buildings in three different European locations, basic tool. *Building and Environment, 51*, 395–401. https://doi.org/10.1016/j.buildenv.2011.11.017

Sair, S., Mandili, B., Taqi, M., & El Bouari, A. (2019). Development of a new eco-friendly composite material based on gypsum reinforced with a mixture of cork fibre and cardboard waste for building thermal insulation. *Composites Communications, 16*, 20–24.

Sartori, I., & Hestnes, A. G. (2007). Energy use in life cycle of conventional and low-energy buildings: A review article. *Energy and Buildings, 39*(3), 249–257. https://doi.org/10.1016/j.enbuild.2006.07.001

Schiavoni, S., D'Alessandro, F., Bianchi, F., & Asdrubali, F. (2016). Insulation materials for building sector: A review and comparative analysis. *Renewable and Sustainable Energy Reviews, 62*, 988–1011. https://doi.org/10.1016/j.rser.2016.05.045

Streimikiene, D., Skulskis, V., Balezentis, T., & Agnusdei, G. P. (2020). Uncertain multi-criteria sustainability assessment of green building insulation materials. *Energy and Buildings, 219*, 110021. https://doi.org/10.1016/j.enbuild.2020.110021

Sun, Y., Wilson, R., & Wu, Y. (2018). A review of transparent insulation material (TIM) for building energy saving and daylight comfort. *Applied Energy, 226*, 713–729.

Tettey, U. Y. A., Dodoo, A., & Gustavsson, L. (2014). Effects of different insulation materials on primary energy and CO2 emission of a multi-storey residential building. *Energy and Buildings, 82*, 369–377. https://doi.org/10.1016/j.enbuild.2014.07.009

Vera, S., Pinto, C., Velasco, P. C., & Bustanmante, W. (2017). Influence of vegetation, substrate, and thermal insulation of an extensive vegetated roof on thermal performance of retail stores in semiarid and marine climates. *Energy and Buildings, 146*, 312–321. https://doi.org/10.1016/j.enbuild.2017.04.037

Wang, C., Zhu, Y., & Guo, X. (2019). Thermally responsive coating on building heating and cooling energy efficiency and indoor comfort improvement. *Applied Energy, 253*, 113506.

Wang, J., Liu, S., Meng, X., Gao, W., & Yuan, J. (2021). Application of retro-reflective materials in urban buildings: A comprehensive review. *Energy and Buildings, 247*, 111137.

Wijesena, G., & Amarasinghe, R. (2018). Solar energy and its role in Sri Lanka. *International Journal of Engineering Trends and Technology (IJETT), 65*(3), 142–148.

Yarbrough, D., Wilkes, K., Olivier, P., Graves, R., & Vohra, A. (2005). *Apparent thermal conductivity data and related information for rice hulls and crushed pecan shells*.

Yuan, J. H., Emura, K., Sakai, H., Farnham, C., & Lu, S. Q. (2016). Optical analysis of glass bead retro-reflective materials for urban heat island mitigation. *Solar Energy, 132*, 203–213.

Yuan, J., Farnham, C., & Emura, K. (2015). Development of a retro-reflective material as building coating and evaluation on albedo of urban canyons and building heat loads. *Energy and Buildings, 103*, 107–117.

Zhang, T., & Yang, H. (2018). Optimal thickness determination of insulating air layers in building envelopes. In *Low carbon cities and urban energy systems*. CUE2018-Applied energy symposium and forum.